



# An analytical model for transient temperature distributions in coated carbide cutting tools<sup>☆</sup>

Shijun Zhang<sup>\*</sup>, Zhanqiang Liu

School of Mechanical Engineering, Shandong University, Jinan, 250061, PR China

## ARTICLE INFO

Available online 13 September 2008

### Keywords:

Transient temperature distributions  
Monolayer coated tools  
Analytical model

## ABSTRACT

The cutting temperature during metal cutting processes has been recognized as one of major factors influencing the tool performance and workpiece geometry accuracy.

This paper presents analyses of the one-dimensional transient temperature distributions in monolayer coated tools. The analytical formulae of the transient temperature distributions for the monolayer cutting tools are obtained using Laplace Transform. Computations of the temperature distributions in monolayer coated tools reveal that such factors as the coating material, substrate material and coating thickness have some influence on temperature distributions in monolayer coated tools. The present work provides some data for selecting appropriate coating materials to reduce temperature within coated tools.

© 2008 Elsevier Ltd. All rights reserved.

## 1. Introduction

In metal cutting operations, the importance of knowledge on the temperature distribution in cutting tool is well recognized due to the severe effects on the tool life and workpiece surface integrity. In general, three regions of intensive heat generation are distinguished, namely the primary deformation zone (shear plane), the tool-chip interface frictional zone or the secondary deformation zone and the tool-workpiece interface zone [1]. The methods to determine temperature in cutting tools include analytical, experimental, numerical (simulation) [2], hybrid technique and heat source methods. Komanduri and Hou [3–5] made a general review of the analytical models about three heat regions and heat conduction in workpiece, chip, and tool. They developed a more appropriate analytical model considering the heat sources from the shear plane, the primary shear zone, and the tool-chip friction interface. They pointed out that the analytical results were in good agreement with the experimental results. They also found that the analytical solutions by using relevant computer program were convenient and more accurate. Wan, Tang and Liu et al. [2] summarized the methods used to measure cutting temperature including tool-work thermocouple, embedded thermocouple, infrared (IR) system, metallographic technique and so on. Then they analyzed the merits and demerits and application ranges of all the methods. Komanduri and Hou [6] also gave a review of the literature on the methods of temperature measurement.

For uncoated tools, the metal cutting temperature has been studied using analytical, numerical, and experimental methods.

Many literatures studied heat conduction in uncoated cutting tools. Komanduri and Hou [6] determined the temperature rise distribution caused by shear plane heat source and friction heat source along the tool-chip interface using the analytical method. Filice, Umbrello and Beccariet al. [7] used 2D thermo-mechanical analysis and 3D pure thermal analysis to simulate machining processes with uncoated cutting tools. The 3D static simulation can be suitable for some applications, but the boundary conditions are the most critical aspect. Rena, Yang and James et al. [8] studied cutting temperatures in hard turning chromium with polycrystalline cubic boron nitride (PCBN) tools using a mixed experimental and finite element simulation. The advantage of this method is that the average temperature at the interface of the insert and the shim can be obtained using a standard thermocouple, making the method attractive for routine measurements. Majumdar, Jayaramachandran and Ganesan [9] used Finite element method to obtain two-dimensional steady state heat diffusion in metal cutting processes. Ng, Aspinwall and Brazil et al. [10] used finite element model to simulate temperature distributions when orthogonal turning a hardened hot work die steel with PCBN tools and validated the model by experimental data from infrared chip surface temperature measurements. They concluded that the tool-chip interface temperature and the chip surface temperature were higher when machining with the low thermal diffusivity PCBN tool than that of with the high thermal diffusivity one. The temperature in the primary shear zone using high thermal conductivity tool was higher than that of using low thermal conductivity tool.

Tool life and cutting speed are extreme important for the productivity of today's industry. In order to improve tool life, much research has been done to reduce cutting temperature in cutting tools. A novel way is using coated cutting tool obtained by means of the deposition of proper coatings on tool surfaces. The coating surfaces of cutting tools have great influence on cutting heat generation and heat

<sup>☆</sup> Communicated by W.J. Minkowycz.

<sup>\*</sup> Corresponding author.

E-mail addresses: [zhangsj.2007@mail.sdu.edu.cn](mailto:zhangsj.2007@mail.sdu.edu.cn) (S. Zhang), [melius@sdu.edu.cn](mailto:melius@sdu.edu.cn) (Z. Liu).

### Nomenclature

$k_1$	thermal conductivity coefficient in coating layer (W/(m. °C))
$k_2$	thermal conductivity coefficient in substrate body of coated tool (W/(m. °C))
$x_1$	thickness of coating layer ( $\mu\text{m}$ )
$x$	spatial coordinates ( $\mu\text{m}$ )
$t$	time (s)
$T^{(1)}$	temperature for coating layer(°C)
$T^{(2)}$	temperature for substrate body(°C)
$T_\infty$	environment temperature (°C) s Laplace operator
$A_1, B_1, A_2, B_2$	constants coefficients
$c$	coefficient defined in Eq. (22)
$n$	integer number (including zero)

### Greek symbols

$\alpha_1$	thermal diffusivity coefficient in coating layer ( $\text{m}^2/\text{s}$ )
$\alpha_2$	thermal diffusivity coefficient in substrate body of coated tool ( $\text{m}^2/\text{s}$ )
$\theta^{(1)}$	temperature for coating layer (°C)
$\theta^{(2)}$	temperature for substrate body (°C)

conduction in tools during machining. The effect of temperature dependent thermal properties may become important for cases when very steep temperature gradient can be generated [11]. So having a more clear understanding about the temperature distributions in coated cutting tools is very useful.

The main methods to determine temperature of coated tools are experimental and numerical methods. The analytical method which was seldom used is obtained by using equivalent layer as a substitute for multilayer coated tools. Grzesik and Nieslony [11] used equivalent parameters of coating layers to calculate tool-chip mean interface temperature and peak temperature, comparing with measured temperature of workpiece and tool thermocouple pair under the condition that cutting speeds were ranging from 100 to 200 m/min. They concluded that the prediction errors for average interface temperature did not exceeded 10–15%. Grzesik and Nieslony [12] used analytical method to predict heat partition coefficient in the stationary tool and in the moving chip with uncoated and multilayer coated tools. Through investigating how the temperature depended on interface temperature, contact length, Peclet number ( $Pe = v_{ch}l_c/\alpha_t$ , where  $v_{ch}$  is sliding chip velocity,  $l_c$  is tool-chip contact length and  $\alpha_t$  denotes coating layer thermal diffusivity) and the specific friction energy, respectively, they found that multilayer coated tool (TiC/Al<sub>2</sub>O<sub>3</sub>/TiN, TiC/Ti(C,N)/Al<sub>2</sub>O<sub>3</sub>/TiN) increased about 30% more heat into chip due to friction. Dessoly, Melkote and Lescalier [13] used finite element method to predict and infrared thermal imaging camera to measure the rake face temperature of the tool (Carbide tool with a TiN coating). They found that the predicted values and the measured values had a good agreement. Grzesik, Bartoszuk and Nieslony [1] used Finite difference method to predict temperature distribution in turning processes with different coated tools. Unfortunately the predicted values and the measurement values have some discrepancies especially with TiC/Al<sub>2</sub>O<sub>3</sub>/TiN coating. In Ref. [14] Finite element, experimental and equivalent parameter methods were used to evaluate temperature distributions within coated tools and tool-chip interface temperatures, respectively. Comparison showed that the simulation results obtained were validated. Du, Lovell and Wu [15] used boundary element method to determine the temperature fields of coated (Al<sub>2</sub>O<sub>3</sub>, TiC, TiN) and uncoated cutting tool inserts. They found that the temperature distributions within cutting tools directly depends on the coating materials and Al<sub>2</sub>O<sub>3</sub> coating has thermal

barrier effect on temperature fields. Grzesik [16] used experiment to investigate the influence of coatings on friction heat generation with different coated tools. He found that coating layers can improve tribological properties of surfaces in sliding contact under employed cutting conditions and some coatings which have thermal barrier effect can substantially reduce contact temperatures. Kwon, Schiemann and Kountanya [17] used an infrared video camera to get chip-tool interface temperature during turning, then used experimental data to determine transient temperature, a one-dimensional ellipsoidal model was constructed to estimate the average steady-state chip-tool interface temperature inversely during turning gray cast iron and AISI 1045 steels with various coated and uncoated K313 carbide inserts. However, the calculated values have much depended on the temperature value which obtained by infrared video camera. Some researchers have predicted temperature distribution or heat flux within coated tools. Kusiak, Battaglia and Rech [18] used heat flux on cutting edge to simulate cutting heat flux on rake face of coated tool inserts. They found that Al<sub>2</sub>O<sub>3</sub> coating led to slight heat flux diminution whereas the other coatings used have no influence on heat flux in coated tools in continuous cutting conditions; nevertheless coatings seem to have thermal resistance in interrupted cutting applications. However, few literatures can be found to display the temperature distributions in coated cutting tools using exact analytical method.

This paper focuses on temperature solution using exact analytical method, and investigates the factors which influence on temperature distributions within monolayer coated cutting tools in transient heat conduction.

## 2. Analytical model

The value of heat flow at the tool and chip interface is difficult to be obtained by measurement method, but the temperature at the tool and chip interface can be measured using some equipment. So the thermal model is established by assuming that the temperature of tool-chip interface is known. Schematic of the thermal model and boundary conditions in one-dimensional coated tools is shown in Fig. 1. The substrate body of coated cutting tools is sufficiently large in the  $x$  direction and can be taken as a semi-infinite body. The temperature at the tool and chip interface is  $T_1$  which is measured in advance. Other outer boundaries of coated tools are assumed to be adiabatic in dry machining, which is reasonable for stagnant-air environment where the free convection in air can be negligible compared to conduction in monolayer coated cutting tools. So the heat dissipation into the tools will deliver only in the coating layer and the substrate of the tools. There is no heat dissipation flowing out through their boundaries. Let  $k_1$  and  $\alpha_1$  be the thermal conductivity and thermal diffusivity of the coating layer, while let  $k_2$  and  $\alpha_2$  be the thermal conductivity and thermal diffusivity of the substrate. Initially ( $t=0$ ), the whole tools are at the environment temperature  $T_\infty$ . This analytical model is similar to that proposed in literature [19], which was used to solve heat conduction problems for the thin-layer medium and an infinite homogeneous medium with concentrated heat sources.

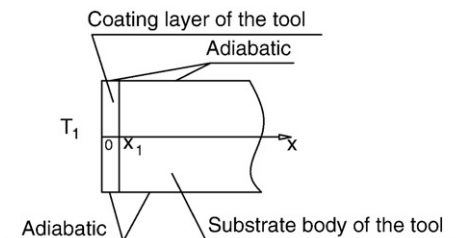


Fig. 1. Schematic of the thermal model and boundary conditions in one-dimensional coated tools.

The following assumptions are made in order to derive the mathematical model of the proposed transient heat conduction process. (a) Thermal properties such as conductivity and diffusivity are independent of temperature and they are uniform for coating layer and substrate body, respectively. (b) The upper and lower surfaces of the coating layer and substrate body are adiabatic. (c) The substrate body is a semi-infinite body in the  $x$  direction as shown in Fig. 1. (d) Perfect thermal contact and no thermal contact resistance occur at the interface  $x=x_1$  between coating layer and substrate body. (e) There is no energy generation within coated tools.

The heat conduction problem under above assumptions can be considered a linear, one-dimensional, and also homogeneous one. Setting  $\theta^{(1)}=T^{(1)}-T_\infty$  in the coating layer, and  $\theta^{(2)}=T^{(2)}-T_\infty$  in the substrate body, the boundary temperature at tool and chip interface  $\theta=T_1-T_\infty$ , the initial ( $t=0$ ) temperature  $\theta^{(1)}=0$  and  $\theta^{(2)}=0$  in the coating and the substrate, respectively, the final mathematical formulae in a Cartesian coordinate system can be given as follows.

- Heat conduction differential equations:

$$\frac{\partial^2 \theta^{(1)}}{\partial x^2} = \frac{1}{\alpha_1} \frac{\partial \theta^{(1)}}{\partial t} \quad 0 \leq x \leq x_1, \quad t \geq 0 \quad (1)$$

$$\frac{\partial^2 \theta^{(2)}}{\partial x^2} = \frac{1}{\alpha_2} \frac{\partial \theta^{(2)}}{\partial t} \quad x_1 \leq x, \quad t \geq 0. \quad (2)$$

- Outer boundary conditions:

$$\theta^{(1)}(x, t) = \theta_1 \quad t \geq 0 \quad (3)$$

$$\theta^{(2)}(x, t) = 0 \quad x \rightarrow \infty, \quad t \geq 0. \quad (4)$$

- Inner boundary (interface between coating and substrate of the tools) conditions:

$$\theta^{(1)}(x_1, t) = \theta^{(2)}(x_1, t) \quad (5)$$

$$-k_1 \frac{\partial \theta^{(1)}}{\partial x} \Big|_{x=x_1} = -k_2 \frac{\partial \theta^{(2)}}{\partial x} \Big|_{x=x_1}. \quad (6)$$

Eq. (5) indicates that the temperatures at the surfaces of separation  $x=x_1$  are identical, which is satisfied the continuity of temperature. Eq. (6) shows that the heat flux is continuous in correspondence to inner boundary surface. The set of Eqs. (1)–(6) will be solved analytically in the next section of this paper.

### 3. Explicit solutions for transient temperature distributions in monolayer coated tools

The physical and mathematic models of coated cutting tools are obtained in the previous section. In this section, the solutions of temperature distribution formulae in monolayer coated tools will be solved. Let the Laplace Transform of  $\theta$  be denoted by

$$\bar{\theta}(x, s) = L[\theta(x, s)] = \int_0^\infty \theta(x, t) e^{-st} dt \quad (7)$$

$$L \left[ \frac{\partial \theta(x, s)}{\partial \tau} \right] = s \bar{\theta}(x, s) - \theta(x, 0) \quad (8)$$

Thus, in Laplace Transform space, the differentials of Eqs. (1)–(6) become

$$\frac{\partial^2 \bar{\theta}^{(1)}}{\partial x^2} - \frac{s}{\alpha_1} \bar{\theta}^{(1)} = 0 \quad 0 \leq x \leq x_1 \quad (9)$$

$$\frac{\partial^2 \bar{\theta}^{(2)}}{\partial x^2} - \frac{s}{\alpha_2} \bar{\theta}^{(2)} = 0 \quad x_1 \leq x \quad (10)$$

$$\bar{\theta}^{(1)} = \frac{\theta_1}{s} \quad x=0 \quad (11)$$

$$\bar{\theta}^{(2)} = 0 \quad x \rightarrow \infty \quad (12)$$

$$\bar{\theta}^{(1)}(x_1, s) = \bar{\theta}^{(2)}(x_1, s) \quad (13)$$

$$-k_1 \frac{\partial \bar{\theta}^{(1)}}{\partial x} \Big|_{x=x_1} = -k_2 \frac{\partial \bar{\theta}^{(2)}}{\partial x} \Big|_{x=x_1} \quad (14)$$

The solution is readily obtained from Eq. (9) as

$$\bar{\theta}^{(1)} = A_1 \exp\left(\sqrt{\frac{s}{\alpha_1}} x\right) + B_1 \exp\left(-\sqrt{\frac{s}{\alpha_1}} x\right). \quad (15)$$

The solution is readily obtained from Eq. (10) as

$$\bar{\theta}^{(2)} = A_2 \exp\left(\sqrt{\frac{s}{\alpha_2}} x\right) + B_2 \exp\left(-\sqrt{\frac{s}{\alpha_2}} x\right) \quad (16)$$

where  $A_1, B_1, A_2, B_2$  are underdetermined constants that are related to the coating layer and substrate body of the tools.

Applying Eq. (15) to satisfy the boundary condition (11), the following result is derived.

$$A_1 + B_1 = \frac{\theta_1}{s} \quad (17)$$

Similarly, Eq. (16) has to satisfy the boundary condition (12); therefore, the following result can be obtained.

$$A_2 = 0 \quad (18)$$

Eqs. (15) and (16) simultaneously satisfy (13) and (14), so Eqs. (13) and (14) become

$$A_1 \exp\left(\sqrt{\frac{s}{\alpha_1}} x_1\right) + B_1 \exp\left(-\sqrt{\frac{s}{\alpha_1}} x_1\right) = A_2 \exp\left(\sqrt{\frac{s}{\alpha_2}} x_1\right) + B_2 \exp\left(-\sqrt{\frac{s}{\alpha_2}} x_1\right) \quad (19)$$

$$k_1 A_1 \sqrt{\frac{s}{\alpha_1}} \exp\left(\sqrt{\frac{s}{\alpha_1}} x_1\right) - k_1 B_1 \sqrt{\frac{s}{\alpha_1}} \exp\left(-\sqrt{\frac{s}{\alpha_1}} x_1\right) = k_2 A_2 \sqrt{\frac{s}{\alpha_2}} \exp\left(\sqrt{\frac{s}{\alpha_2}} x_1\right) - k_2 B_2 \sqrt{\frac{s}{\alpha_2}} \exp\left(-\sqrt{\frac{s}{\alpha_2}} x_1\right) \quad (20)$$

The results of the coefficients  $A_1, B_1, A_2, B_2$  in Eqs. (15) and (16) can be derived by solving the Eqs. (17), (18), (19), and (20)

$$A_1 = \frac{\frac{\theta_1 c}{s} \exp\left(-2\sqrt{\frac{s}{\alpha_1}} x_1\right)}{1 - c \cdot \exp\left(-2\sqrt{\frac{s}{\alpha_1}} x_1\right)} \frac{q_0 \sqrt{\alpha_1}}{k_1} \quad (21)$$

where  $c$  is given by

$$c = \frac{k_1 \sqrt{\alpha_2} - k_2 \sqrt{\alpha_1}}{k_1 \sqrt{\alpha_2} + k_2 \sqrt{\alpha_1}} \quad (22)$$

Because the term  $\exp\left(-2\sqrt{\frac{s}{\alpha_1}}x_1\right)$  is in the denominator of Eq. (21), it is impossible to invert the Laplace Transform directly. The Taylor series expansion is used which results

$$A_1 = \frac{\theta_1}{s} \sum_{n=0}^{\infty} \left\{ (\pm 1)^n c^{n+1} \exp\left[-2(n+1)\sqrt{\frac{s}{\alpha_1}}x_1\right] \right\} \quad (23)$$

$$B_1 = \frac{\theta_1}{s} - A_1 \quad (24)$$

$$B_2 = \frac{\theta_1}{s} \exp\left(-\sqrt{\frac{s}{\alpha_1}}x_1 + \sqrt{\frac{s}{\alpha_2}}x_1\right) + A_1 \exp\left(\sqrt{\frac{s}{\alpha_1}}x_1 + \sqrt{\frac{s}{\alpha_2}}x_1\right) - A_1 \exp\left(-\sqrt{\frac{s}{\alpha_1}}x_1 + \sqrt{\frac{s}{\alpha_2}}x_1\right) \quad (25)$$

So the coefficients of  $A_1, B_1, A_2, B_2$  in Eqs. (15) and (16) have been obtained. By taking the Inversion of Laplace Transform of Eqs. (15) and (16) and applying the results to Eqs.  $\theta^{(1)} = T^{(1)} - T_{\infty}$  and  $\theta^{(2)} = T^{(2)} - T_{\infty}$ , respectively, the exact full-field transient temperature distribution in the monolayer coated tool can be expressed as follows.

$$T^{(1)} = \theta_1 \sum_{n=0}^{\infty} \left\{ (\pm 1)^n c^{n+1} \operatorname{erfc}\left[\frac{2(n+1)\sqrt{\frac{1}{\alpha_1}}x_1 - \sqrt{\frac{1}{\alpha_1}}x}{2t}\right] \right\} + \theta_1 \operatorname{erfc}\left(\frac{\sqrt{\frac{1}{\alpha_1}}x}{2t}\right) - \theta_1 \sum_{n=0}^{\infty} \left\{ (\pm 1)^n c^{n+1} \operatorname{erfc}\left[\frac{2(n+1)\sqrt{\frac{1}{\alpha_1}}x_1 + \sqrt{\frac{1}{\alpha_1}}x}{2t}\right] \right\} + T_{\infty} \quad (26)$$

$$T^{(2)} = \theta_1 \operatorname{erfc}\left(\frac{\sqrt{\frac{1}{\alpha_1}}x_1 - \sqrt{\frac{1}{\alpha_2}}x_1 + \sqrt{\frac{1}{\alpha_2}}x}{2t}\right) + \theta_1 \sum_{n=0}^{\infty} \left\{ (\pm 1)^n c^{n+1} \operatorname{erfc}\left[\frac{(2n+1)\sqrt{\frac{1}{\alpha_1}}x_1 - \sqrt{\frac{1}{\alpha_2}}x_1 + \sqrt{\frac{1}{\alpha_2}}x}{2t}\right] - \operatorname{erfc}\left[\frac{(2n+3)\sqrt{\frac{1}{\alpha_1}}x_1 - \sqrt{\frac{1}{\alpha_2}}x_1 + \sqrt{\frac{1}{\alpha_2}}x}{2t}\right] \right\} + T_{\infty} \quad (27)$$

In Eqs. (23)–(27) the positive sign is valid when  $c > 0$ , while the negative sign is valid when  $c < 0$ .

**4. Computations and discussions**

By using the analytical explicit solutions developed in the previous sections, calculations of transient temperature distributions are obtained

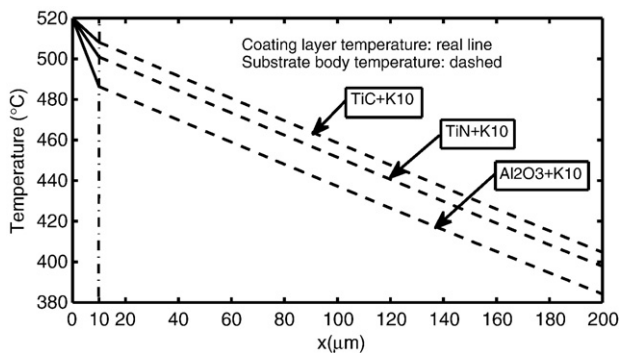


Fig. 2. Influences of coating material on temperature distribution within the coating/substrate.

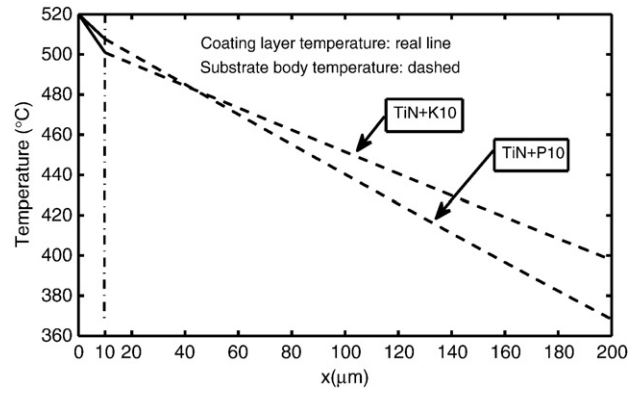


Fig. 3. Influences of tool substrate material on temperature distribution within the coating/substrate.

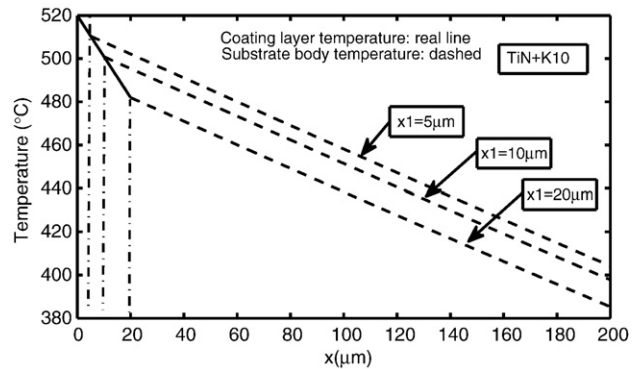


Fig. 4. Influence of coating thickness on temperature distribution within the coating/substrate.

for monolayer coated cutting tools via a computational program with formulae (26), (27). In order to investigate heat isolating effect of different materials, the temperature distributions for carbide tools coated with several coatings (TiN, TiC and  $Al_2O_3$ ) and two substrates (K10 and P10) are considered for the calculations. The full-field results displayed in Figs. 2–4. The prediction is transient temperatures in coated tools during dry cutting. It means that the values of temperature determined in coated tools are varied depending on the cutting time. In order to investigate temperature distribution at a certain time,  $t = 0.1$  s was selected in the following investigation. X axis in all the figures from 2 to 4 indicates the distance from the coating surface, and the y axis represents temperature. The temperature at  $x = 0$  was assumed  $T_1 = 520$  °C. The environment temperature was kept at 20 °C. Thickness of the coating layer was selected  $x_1 = 10 \mu m$  ( $1 \times 10^{-5}$  m) except in Fig. 4. Due to the coating temperatures in the examples are about 500 °C, the parameters of coating layer and substrate body of the cutting tools at 500 °C were selected (Table 1).

All the temperature distribution curves show the similar decreasing trend in monolayer coated cutting tools with the increase of the x

Table 1 Selected physical properties of coatings and substrates in the examples

	Material	Thermal conductivity $k_1$ or $k_2$ / (W/(m °C))	Thermal diffusivity $\alpha_1$ or $\alpha_2$ / ( $m^2/s$ )
Coating layer	Titanium carbide (TiC)	23	$7.667 \times 10^{-6}$
	Titanium nitride (TiN)	37	$1.45 \times 10^{-5}$
	Aluminum oxide ( $Al_2O_3$ )	13	$3.186 \times 10^{-6}$
Substrate	ISO K10	79.5	$2.6 \times 10^{-6}$
	ISO P10	37.7	$1.4 \times 10^{-6}$



coordinate. In order to illustrate clearly, the figures are displayed only at the range from  $x=0$  to  $x=200\ \mu\text{m}(2\times 10^{-4}\ \text{m})$ . In the full-field distribution contours, solid lines and dashed lines are used to indicate temperature values in coatings and substrates, respectively. Fig. 2 depicted the temperature distributions in coated tools with different coatings and same substrate. It shows that the temperature distributions in monolayer coated tools are different with different coating layers. Whereas, Fig. 3 displayed the temperature distributions in TiN coated tools with different substrates (K10, P10). It shows that temperature fields used TiN coating layer and different substrates are different. Fig. 4 depicted the temperature fields in coated tools with different thickness of  $5\ \mu\text{m}$ ,  $10\ \mu\text{m}$  and  $20\ \mu\text{m}$  coating layers at  $t=0.1\ \text{s}$ . It shows that the temperature rises in monolayer coated tools are different with various thickness coating layers.

Fig. 2 indicates that the thermophysical properties of coatings have a significant influence on temperature rise within coating and substrate of coated tools. Fig. 3 shows that the thermophysical properties of substrates can not only influence temperature distribution in substrate but also in coating of coated tools. This finding gives evidence that both coating and substrate must be taken into account when one selecting cutting tool in machining process. The comparisons in Fig. 2 reveals that the  $\text{Al}_2\text{O}_3$  coating with K10 substrate produces relatively lower temperatures both in the coating and substrate of coated tools at the same  $x$  coordinate. The high temperatures within substrates are  $508.1\ ^\circ\text{C}$ ,  $501.0\ ^\circ\text{C}$  and  $486.3\ ^\circ\text{C}$  with TiC, TiN and  $\text{Al}_2\text{O}_3$  coating layers, respectively. Those results show that  $\text{Al}_2\text{O}_3$  coating is more effective than TiC and TiN in diminishing temperature in coated tools during cutting. The reason is that the  $\text{Al}_2\text{O}_3$  coating material has lower coefficient of thermal conductivity. In fact, the temperature distribution depends on two coefficients combined effect, namely, the coefficients of thermal conductivity and thermal diffusivity. Du, Lovell and Wu [15] predicted similar result that  $\text{Al}_2\text{O}_3$  coating has thermal barrier effect using boundary element method. From the depiction in Fig. 4, it shows that coating thickness also has some influence on temperature rise. The temperatures are  $502.1\ ^\circ\text{C}$ ,  $495.4\ ^\circ\text{C}$  and  $482.0\ ^\circ\text{C}$  at  $x=20\ \mu\text{m}$  with  $5\ \mu\text{m}$ ,  $10\ \mu\text{m}$  and  $20\ \mu\text{m}$  thickness of TiN coating layer, respectively. The temperature difference is  $20.1\ ^\circ\text{C}$  with  $5\ \mu\text{m}$  and  $20\ \mu\text{m}$  thickness of TiN coating layer with the substrate of K10. The result is similar with the previous work in literature [15], in which the authors predicted the temperature difference is about  $55\ ^\circ\text{C}$  with different coating thickness from  $1\ \mu\text{m}$  to  $50\ \mu\text{m}$ .

## 5. Conclusions

In this paper, an analytical model with constant temperature at tool and chip interface of one-dimensional heat transfer in monolayer coated tools has been developed to investigate temperature distribution in metal cutting. The explicit form of temperature formulae were obtained by using the Laplace Transform technique and a Taylor series expansion. Calculations conducted for tools of three coatings (TiN, TiC and  $\text{Al}_2\text{O}_3$ ) and two substrates (K10 and P10). The transient temperature distributions have shown that the thermophysical parameters of coating and substrate materials have huge influences on temperature distributions in monolayer coated tools. The analytical solution method has demonstrated that  $\text{Al}_2\text{O}_3$  coating has more effective thermal barrier effect than the other two coating materials.

The coating thickness also has some influence on temperature distributions in coated tools. The present work would be valuable for selecting coating materials in metal cutting process.

## Acknowledgements

This project is supported by National Natural Science Foundation of China (50675122), Excellent Postdoctoral Foundation of Shandong Province (200602008), and the Program for New Century Excellent Talents in University (NCET-04-0629).

## References

- [1] W. Grzesik, M. Bartoszek, P. Nieslony, Finite difference analysis of the thermal behaviour of coated tools in orthogonal cutting of steels, *International Journal of Machine Tools & Manufacture* 44 (2004) 1451–1462.
- [2] Y. Wan, Z.T. Tang, Z.Q. Liu, X. Ai, The assessment of cutting temperature measurements in high-speed machining, in *Materials Science Forum* 2004.
- [3] R. Komanduri, Z.B. Hou, Thermal modeling of the metal cutting process. Part I: temperature rise distribution due to shear plane heat source, *International Journal of Mechanical Sciences* 42 (2000) 1715–1752.
- [4] R. Komanduri, Z.B. Hou, Thermal modeling of the metal cutting process. Part II: temperature rise distribution due to frictional heat source at the tool-chip interface, *International Journal of Mechanical Sciences* 43 (2001) 57–88.
- [5] R. Komanduri, Z.B. Hou, Thermal modeling of the metal cutting process. Part III: temperature rise distribution due to the combined effects of shear plane heat source and the tool-chip interface frictional heat source, *International Journal of Mechanical Sciences* 43 (2001) 89–107.
- [6] R. Komanduri, Z.B. Hou, A review of the experimental techniques for the measurement of heat and temperatures generated in some manufacturing processes and tribology, *Tribology International* 34 (2001) 653–682.
- [7] L. Filice, F. Micari, S. Rizzuti, D. Umbrello, A critical analysis on the friction modelling in orthogonal machining, *International Journal of Machine Tools & Manufacture* 47 (2007) 709–714.
- [8] X.J. Ren, Q.X. Yang, R.D. James, L. Wang, Cutting temperatures in hard turning chromium hardfacings with PCBN tooling, *Journal of Materials Processing Technology* 147 (2004) 38–44.
- [9] P. Majumdar, R. Jayaramachandran, S. Ganesan, Finite element analysis of temperature rise in metal cutting processes, *Applied Thermal Engineering* 25 (2005) 2152–2168.
- [10] E.-. Ng, D.K. Aspinwall, D. Brazil, J. Monaghan, Modelling of temperature and forces when orthogonally machining hardened steel, *International Journal of Machine Tools & Manufacture* 39 (1999) 885–903.
- [11] W. Grzesik, P. Nieslony, Physics based modelling of interface temperatures in machining with multilayer coated tools at moderate cutting speeds, *International Journal of Machine Tools & Manufacture* 44 (2004) 889–901.
- [12] W. Grzesik, P. Nieslony, A computational approach to evaluate temperature and heat partition in machining with multilayer coated tools, *International Journal of Machine Tools & Manufacture* 43 (2003) 1311–1317.
- [13] V. Dessoly, S.N. Melkote, C. Lescahier, Modeling and verification of cutting tool temperatures in rotary tool turning of hardened steel, *International Journal of Machine Tools & Manufacture* 44 (2004) 1463–1470.
- [14] W. Grzesik, Determination of temperature distribution in the cutting zone using hybrid analytical-FEM technique, *International Journal of Machine Tools & Manufacture* 46 (2006) 651–658.
- [15] F. Du, M.R. Lovell, T.W. Wu, Boundary element method analysis of temperature fields in coated cutting tools, *International Journal of Solid and Structures* 38 (2001) 4557–4570.
- [16] W. Grzesik, The influence of thin hard coatings on frictional behaviour in the orthogonal cutting process, *Tribology International* 33 (2000) 131–140.
- [17] P. Kwon, T. Schiemann, R. Kountanya, An inverse estimation scheme to measure steady-state tool-chip interface temperatures using an infrared camera, *International Journal of Machine Tools & Manufacture* 41 (2001) 1015–1030.
- [18] A. Kusiak, J. Battaglia, J. Rech, Tool coatings influence on the heat transfer in the tool during machining, *Surface & Coatings Technology* 195 (2005) 29–40.
- [19] Analytical investigations for heat conduction problems in anisotropic thin-layer media with embedded heat sources, *International Journal of Heat and Mass Transfer* 45 (2002) 4117–4132.